RESEARCH FRONT

CSIRO PUBLISHING

Aust. J. Chem. **2017**, *70*, 373–386
http://dx.doi.org/10.1071/CH16587

Full Paper

Syntheses, Structural Studies, and Copper Iodide Complexes of Macrocycles Derived from Williamson Ether Syntheses Involving 2,9-Bis(4-hydroxyphenyl)-1,10-phenanthroline, α,ω-Dibromides, and Resorcinol or 2,7-Dihydroxynaphthalene

Zuzana Baranová,[A] *Hashem Amini,*[A] *Madhav Neupane,*[A] *Sydney C. Garrett,*[A] *Andreas Ehnbom,*[A] *Nattamai Bhuvanesh,*[A] *Joseph H. Reibenspies,*[A] *and John A. Gladysz*[A,B]

[A]Department of Chemistry, Texas A&M University, PO Box 30012, College Station, Texas 77843-3012, USA.
[B]Corresponding author. Email: gladysz@mail.chem.tamu.edu

1,3-Bis(6-bromohexyloxy)benzene, 2,7-bis(6-bromohexyloxy)naphthalene, 1,3-bis(4-bromomethylbenzyloxy)benzene, and 1,3-bis(3-bromomethylbenzyloxy)benzene were prepared via Williamson ether synthesis using resorcinol or 2,7-dihydroxynaphthalene and 1,6-dibromohexane, 1,4-bis(bromomethyl)benzene, or 1,3-bis(bromomethyl)benzene (21–47 % yield). These dibromides were condensed with 2,9-bis(4-hydroxyphenyl)-1,10-phenanthroline in the presence of K_2CO_3 to give the corresponding 31- to 35-membered macrocycles (**3a**–**d**, 22–63 % yield). When **3a**–**d** were treated with CuI, mononuclear 1 : 1 complexes formed, in which the CuI chelates to the nitrogen donor atoms of the phenanthroline moiety (**4a**–**d**, 40–80 % yield). The crystal structures of **3a**–**c** and **4a**–**c** were determined and analyzed using density functional theory calculations and in the context of rotaxanes that could be formed by treatment of **4a**–**d** with terminal alkynes (e.g. macrocycle dimensions, void volumes). The copper and iodide atoms in **4a**–**c** significantly protrude from the least-squares plane of the phenanthroline moiety (0.46–0.63 Å and 1.65–2.07 Å).

Manuscript received: 14 October 2016.
Manuscript accepted: 16 November 2016.
Published online: 23 December 2016.

Introduction

Macrocycles and metal complexes thereof play ubiquitous roles in supramolecular chemistry and particularly the synthesis of mechanically interlocked molecules (MIMs),[1] a descriptor that encompasses catenanes, rotaxanes, and knots.[2,3] Variables such as shape, conformational flexibility, and the nature and position of functional groups can influence the efficacy of these processes and the properties of the topologically novel products.[4]

In ongoing efforts, we have sought to synthesize rotaxanes derived from diplatinum polyynediyl axles and 2,9-disubstituted 1,10-phenanthroline-based macrocycles, as exemplified by **I** in Scheme 1.[5,6] The former building blocks have been the subject of extensive studies in our laboratory.[7] Such complexes are normally accessed by oxidative homocouplings of the corresponding monoplatinum polyynyl complexes under 'Hay conditions' (O_2, CuCl/tetramethylethylenediamine).[8]

The latter building blocks have been applied to MIMs by several groups.[4d,9–11] The inspiration for our studies came from Saito et al., who employed CuI complexes with polyether $O(CH_2)_mO$ ($m = 6, 8$) and *m*-C_6H_4 linkages to prepare rotaxanes with organic 1,3-butadiyne axles, as exemplified by **II** in Fig. 1.[10] The copper(I) 1,10-phenanthroline precursors represent an embodiment of the 'active metal template' strategy popularized by Leigh et al.[4d,e,g,12] In this scenario, the copper is believed to template the coupling partners onto opposite faces of the macrocycle complex, thereby facilitating subsequent elimination to a rotaxane topology.

Accordingly, in this paper we describe (1) the preparation of three new and one previously reported 2,9-disubstituted 1,10-phenanthroline based macrocycles, (2) the synthesis of the corresponding CuI complexes, (3) crystallographic and density functional theory (DFT) characterization of the macrocycles and complexes, and (4) analyses of their geometries, particularly features relevant to the derived rotaxanes and their proposed mechanism of formation. Portions of the preparative chemistry and one crystal structure have been described in the Supplementary Material of preliminary communications.[5,6] The resulting rotaxanes will be the subject of a subsequent full paper.[13]

Results

Synthesis of Macrocycles

We sought a family of polyether macrocycles based on a 2,9-disubstituted 1,10-phenanthroline 'northern hemisphere' and a dihydroxyarene-derived 'southern hemisphere' with a gradation

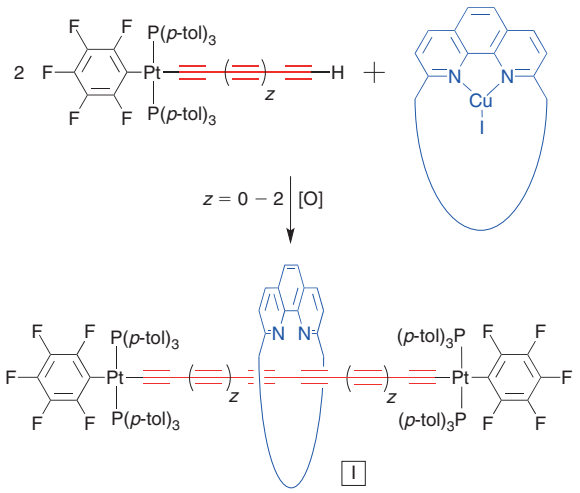

Scheme 1. Rotaxanes derived from diplatinum polyynediyl axles and 1,10-phenanthroline-based macrocycles (**I**).

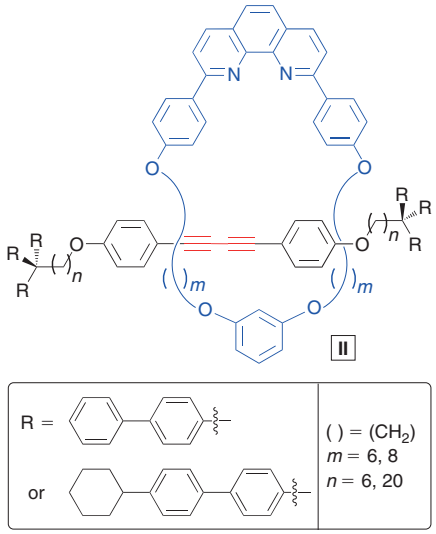

Fig. 1. Rotaxanes synthesized by Saito et al. via oxidative homocouplings of organic terminal monoalkynes using CuI complexes of 1,10-phenanthroline-containing macrocycles.[10d,e,14]

of dimensions and conformational degrees of freedom. The first target molecule had been previously reported by Saito et al. as part of their study in Fig. 1,[10a] and the synthetic route is summarized in Scheme 2 (top).[14] The 'northern' precursor **1** was easily accessed via a two-step sequence starting with 1,10-phenanthroline and 4-lithioanisole.[9a,15]

As with all of the preparations described below, the 'southern' precursor was accessed by a classical Williamson ether synthesis. Thus, resorcinol, 1,6-dibromohexane, and K_2CO_3 were allowed to react in acetone (1.0 : 3.0 : 2.5 mole ratio). A chromatographic workup gave the diether **2a**[16] as a white solid in 47 % yield. Then, **1**, **2a**, and K_2CO_3 were combined in wet DMSO (1.0 : 1.0 : 14.0 mole ratio). Workup gave **3a**, which features a 33-membered ring in 59 % yield as an air stable white solid (literature: 41 %).[14] In cases where we improved on reported yields and/or acquired new NMR data, experimental details are provided in the Supplementary Material.

In the second target molecule, the previously unknown **3b** (Scheme 2, bottom), the resorcinol unit of **3a** was replaced by a 2,7-dihydroxynaphthalene moiety, thereby expanding the macrocycle cavity to a 35-membered ring. A reaction between 2,7-dihydroxynaphthalene, 1,6-dibromohexane, and K_2CO_3 (1.0 : 3.0 : 2.5 mole ratio) in acetone gave the 'southern' precursor **2b** as a white solid in 41 % yield. Condensation of **1**, **2b**, and K_2CO_3 (1.0 : 1.0 : 14.0 mole ratio) then afforded **3b** as a white solid in 63 % yield. The products **2b** and **3b**, and all other new compounds below were characterized by NMR spectroscopy (^{1}H and ^{13}C{^{1}H}) and microanalyses, as summarized in the Experimental section.

In the third target molecule, the previously unknown **3c** (Scheme 3, top), the $(CH_2)_6$ linker of **3a** was replaced by a more rigid *p*-xylylyl moiety, which maintains a 33-membered ring. Reaction between resorcinol, 1,4-bis(bromomethyl)benzene, and K_2CO_3, similar to the analogous condensations above, gave the 'southern' precursor **2c** in 21 % yield. This was followed by reaction between **1**, **2c**, and K_2CO_3 (1.0 : 1.0 : 3.0 mole ratio), which afforded **3c** in 39 % yield. In the final target molecule, **3d** (Scheme 3, bottom), the *p*-xylylyl moiety of **3c** was replaced by a *m*-xylylyl linkage, reducing the ring size to 31. An analogous sequence gave **2d** in 38 % yield and **3d** in 22 % yield. All of the new organic compounds in Scheme 3 were white or pale yellow solids.

Several related macrocyclic targets were contemplated. In the course of a vigorous program involving undergraduate research students, additional 'southern' precursors were prepared (e.g. analogues of **2c**, **d** derived from 2,7-dihydroxynaphthalene). For a variety of reasons, the macrocycle syntheses were not completed. Nonetheless, new compounds that were completely characterized are included in the Supplementary Material.

Copper(I) Complexes

In accord with the preparative goals in the introduction, copper(I) complexes of the macrocycles were sought. Various copper halides were screened, and copper(I) iodide proved to be optimal in terms of yield and product stability. Thus, as shown in Schemes 2 and 3, CH_2Cl_2 solutions of the macrocycles **3a**–**d** were combined with acetonitrile solutions of CuI. Workups gave the 1 : 1 adducts **4a**–**d** in 40–80 % yields as orange-to-yellow crystals or solids that were stable to >100°C.[17]

Spectroscopic and Structural Characterization

The NMR properties of the macrocycles (see Experimental section) were unremarkable , but nonetheless important in providing baselines for shielding effects in the corresponding rotaxanes.[5,13] The CuI complexes with the xylylyl linkers, **4c**, **d**, were poorly soluble, and good quality spectra could not be obtained. With **4a**, **b**, some of the phenanthroline ^{1}H NMR signals were 0.1–0.2 ppm downfield from those of **3a**, **b**. In contrast, the *p*-C_6H_4 protons that were *ortho* to the phenanthroline shifted upfield by 0.27–0.34 ppm. Some signals also broadened.

Crystals of **3a** and the solvates **3b**·2$CHCl_3$ and **3c**·CH_2Cl_2 could be grown as described in the Experimental section. The crystal structures were solved as summarized in Table 1 and the Experimental section. Out of all the solvate molecules, only one of the two associated with **3b** could be accurately modelled. The others were removed during refinement using standard protocols, and thus do not appear in the headers in the tables. Key metrical parameters are given in Table 2.[18]

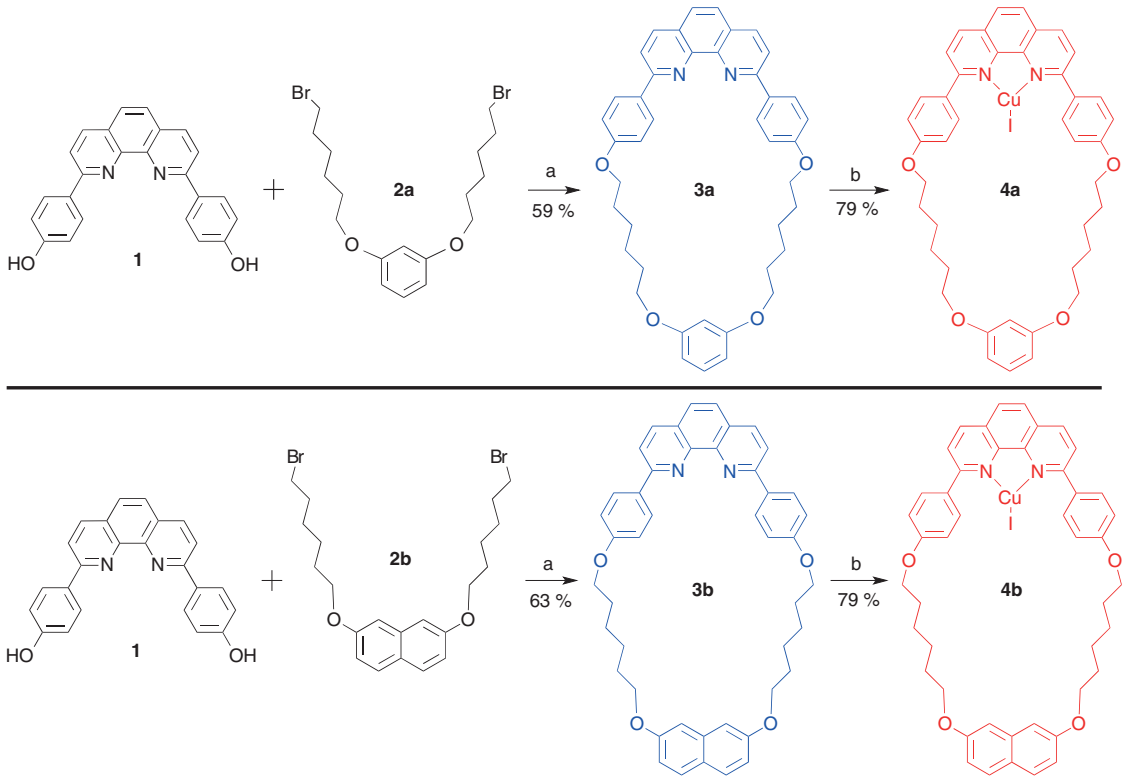

Scheme 2. Syntheses of macrocycles containing $O(CH_2)_6O$ tethers and copper complexes thereof: (a) K_2CO_3, wet DMSO; (b) CuI, CH_3CN/CH_2Cl_2.

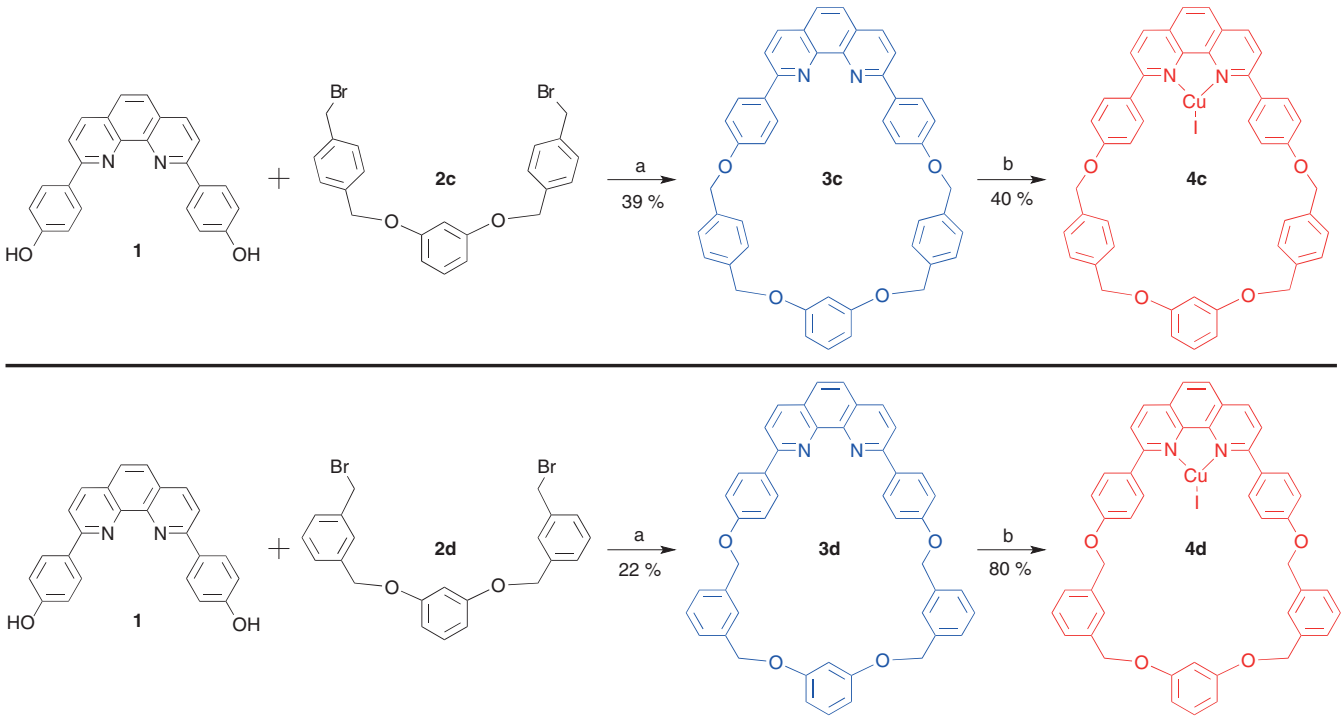

Scheme 3. Syntheses of macrocycles containing $OCH_2C_6H_4CH_2O$ tethers and copper complexes thereof: (a) K_2CO_3, wet DMSO; (b) CuI, CH_3CN/CH_2Cl_2.

Thermal ellipsoid plots and space filling representations of **3a**–**c** are provided in Fig. 2. The molecular structure of **3c** exhibited a mirror plane that bisected the resorcinol and central phenanthroline rings, as consistent with the space group *Pnma*. In contrast, **3a**, **b** crystallized in chiral conformations with both enantiomers in the unit cell. Deviating from usual procedures, the symmetry equivalent atoms of **3c** were assigned different numbers (see Fig. 3),[18] similar to those of the analogous atoms

Table 1. Crystallographic data for 3a–c

	3a[A]	**3b**·$CHCl_3$[B]	**3c**[B]
Empirical formula	$C_{42}H_{42}N_2O_4$	$C_{47}H_{45}Cl_3N_2O_4$	$C_{46}H_{34}N_2O_4$
Formula weight	638.78	808.20	678.75
Temperature [K]	110(2)	110(2)	110(2)
Wavelength [Å]	1.54178	1.54178	0.71073
Diffractometer	Bruker D8 GADDS	Bruker D8 GADDS	Bruker APEX 2
Crystal system	Monoclinic	Triclinic	Orthorhombic
Space group	*Pn*	*P*-1	*Pnma*
Unit cell dimensions			
a [Å]	10.8861(9)	8.4044(4)	11.058(4)
b [Å]	15.6003(14)	14.7638(6)	23.613(8)
c [Å]	11.1600(10)	18.7247(8)	14.049(5)
α [°]	90	73.146(3)	90
β [°]	112.189(4)	85.741(3)	90
γ [°]	90	81.873(3)	90
Volume [$Å^3$]	1754.9(3)	2199.89(17)	3668(2)
Z	2	2	4
ρ_{calcd} [Mg m^{-3}]	1.209	1.220	1.229
μ [mm^{-1}]	0.611	2.231	0.078
F(000)	680	848	1424
Crystal size [mm^3]	0.11 × 0.10 × 0.03	0.12 × 0.06 × 0.04	0.12 × 0.10 × 0.07
Range for data collection	2.83 to 59.99	2.47 to 60.00	2.34 to 24.99
Index ranges	$-12 \le h \le 12$	$-9 \le h \le 9$	$-13 \le h \le 13$
	$-17 \le k \le 17$	$-16 \le k \le 16$	$-28 \le k \le 28$
	$-12 \le l \le 12$	$-21 \le l \le 21$	$-16 \le l \le 16$
Reflections collected	24948	43282	33095
Independent reflections	4608 ($R_{int} = 0.0499$)	6414 ($R_{int} = 0.0526$)	3286 ($R_{int} = 0.0504$)
Max. and min. transmission	0.9819 and 0.9358	0.9161 and 0.7756	0.9945 and 0.9906
Data / restraints / parameters	4608 / 2 / 434	6414 / 6 / 525	3286 / 0 / 239
Goodness-of-fit on F^2	0.990	1.064	1.032
Final *R* indices [$I > 2\sigma(I)$]	$R1 = 0.0364$	$R1 = 0.0519$	$R1 = 0.0401$
	$wR2 = 0.0832$	$wR2 = 0.1416$	$wR2 = 0.1031$
R indices (all data)	$R1 = 0.0459$	$R1 = 0.0619$	$R1 = 0.0486$
	$wR2 = 0.0900$	$wR2 = 0.1477$	$wR2 = 0.1073$
Largest diff. peak and hole [e$Å^{-3}$]	0.208 and −0.193	0.605 and −0.553	0.169 and −0.155

[A]This structure was described earlier in reference [6].
[B]Some or all of the solvate molecules were removed during refinement as described in the Experimental section.

of **3a**, **b**. This facilitates comparisons of metrical parameters (Table 2). The oxygen lone pairs in **3b**, **c** and most of those in **3a** were *exo* to the macrocycle cavity, analogous to the dominant orientation in the corresponding rotaxanes.[5]

Crystals of solvates of the corresponding CuI complexes – **4a**·CH_2Cl_2, **4b**·2$CHCl_3$, and **4c**·CH_2Cl_2 – were also obtained. These structures were similarly solved, giving the representations in Fig. 3 and metrical parameters in Table 2.[18] In all cases, the solvent molecules could be accurately modelled. The oxygen lone pairs in **4b**, **c** and most of those in **4a** were *exo* to the macrocycle cavity, paralleling the situation with **3a**–**c**.

The copper atoms of **4a**–**c** exhibited distorted trigonal planar coordination geometries, with the N–Cu–N bond angles (82.46(14)°–83.17(10)°) being much smaller than the N–Cu–I bond angles (133.86(8)°–140.52(10)°). The sums of the three bond angles (355.51°–357.11°; see Table 2) were close to 360°. In all cases, the CuI moieties markedly protruded on one side of the planar $C_{12}N_2$ 1,10-phenanthroline units. The distances of the copper and iodide atoms from the phenanthroline least-squares planes ranged from 0.46 to 0.63 Å and from 1.65 to 2.07 Å, respectively (Table 2). The $CuIN_2$ units were roughly planar (maximum atomic deviations from least-squares planes: 0.14–0.15 Å). Thus, the folding angles with the phenanthroline least-squares planes were calculated and ranged from 24.3° to 31.0°.

In all of the solvates that could be crystallographically modelled (**3b** in part; **4a**–**c**), solvent was found in the macrocycle cavity. Some representative motifs are depicted in Fig. 4. However, bonding interactions with the macrocycle or CuI moiety were not apparent. In **3a**, intermolecular N···HC hydrogen bonds were present, as depicted in the Supplementary Material (Fig. S2). In **4a**–**c**, π stacking interactions were also obvious (Figs S3–S5). Additional analyses of the structural data are provided in the Discussion section.

The compounds in Figs. 2 and 3 were also modelled by DFT calculations as described in the Experimental section. In all cases, the optimized geometries very closely corresponded to those found in the crystals. The similarities were so striking that these data are simply represented by overlays in the Supplementary Material (Figures S8–S10). In particular, the CuI moieties were again displaced from the planes of the 1,10-phenanthroline units. The distances of the copper and iodide atoms from the least-squares planes ranged from 0.51 to 0.57 Å and from 1.69 to 1.86 Å, respectively (folding angles 24.4°-26.8°).

Analogous calculations were also carried out with **3d** and **4d**, and analogues of **3c**, **d** and **4c**, **d** in which the 'southern hemispheres' were derived from 2,7-dihydroxynaphthalene as opposed to resorcinol (species not yet synthesized). Given the excellent agreement of theory and experiment with **3a**–**c** and

Table 2. Key crystallographic distances (Å), angles (°), and void volumes (Å^3) for 3a–c and 4a–c

	3a[A]	**3b**·$CHCl_3$[B]	**3c**[B]	**4a**·CH_2Cl_2	**4b**·$2CHCl_3$	**4c**·CH_2Cl_2
Cu–N1	–	–	–	2.077(3)	2.053(3)	2.059(3)
Cu–N2	–	–	–	2.051(4)	2.054(2)	2.072(3)
Cu–I	–	–	–	2.4306(7)	2.4347(8)	2.4325(5)
C1–N1	1.330(3)	1.332(3)	1.321(2)	1.346(6)	1.346(6)	1.338(4)
N1–C5	1.357(3)	1.358(3)	1.3581(19)	1.373(6)	1.373(6)	1.369(5)
C5–C9	1.448(4)	1.457(4)	1.450(3)	1.437(6)	1.437(6)	1.443(5)
C9–N2	1.356(3)	1.364(3)	1.3581(19)	1.370(5)	1.370(5)	1.358(5)
N2–C12	1.338(3)	1.336(3)	1.321(2)	1.349(5)	1.349(5)	1.344(5)
C12–C13	1.481(4)	1.483(4)	1.492(2)	1.478(6)	1.473(5)	1.474(6)
C16–O1	1.373(3)	1.365(3)	1.3808(18)	1.364(5)	1.361(4)	1.375(5)
O1–C19	1.438(3)	1.442(3)	1.432(2)	1.443(5)	1.433(4)	1.427(5)
C19–C20	1.501(4)	1.505(4)	1.507(2)	1.494(6)	1.493(5)	1.506(6)
C20–C21	1.511(4)	1.529(4)	1.390(2)/1.382(2)[C]	1.530(6)	1.521(5)	1.390(6)/1.390(6)[C]
C21–C22	1.508(4)	1.533(4)	1.386(2)/1.393(2)[C]	1.528(6)	1.515(5)	1.387(6)/1.383(6)[C]
C22–C23	1.533(4)	1.528(4)	1.390(2)/1.389(2)[C]	1.528(6)	1.522(4)	1.394(6)/1.391(6)[C]
C23–C24	1.503(4)	1.505(4)	1.513(2)	1.501(6)	1.509(4)	1.495(6)
C24–O2	1.435(3)	1.445(3)	1.4243(18)	1.439(5)	1.431(4)	1.432(5)
O2–C25	1.385(3)	1.367(3)	1.3761(17)	1.376(5)	1.367(4)	1.381(5)
C29–O3	1.376(3)	1.372(3)	1.3761(17)	1.374(5)	1.365(4)	1.368(5)
O3–C31	1.440(3)	1.431(3)	1.4243(18)	1.445(5)	1.427(4)	1.445(5)
C31–C32	1.505(4)	1.507(4)	1.513(2)	1.513(6)	1.516(5)	1.505(6)
C32–C33	1.521(3)	1.534(4)	1.390(2)/1.389(2)[C]	1.516(6)	1.517(4)	1.399(6)/1.371(6)[C]
C33–C34	1.528(4)	1.516(4)	1.386(2)/1.393(2)[C]	1.528(6)	1.528(4)	1.374(6)/1.398(6)[C]
C34–C35	1.524(3)	1.521(4)	1.390(2)/1.382(2)[C]	1.526(6)	1.502(4)	1.408(6)/1.366(6)[C]
C35–C36	1.500(4)	1.501(4)	1.507(2)	1.524(6)	1.520(4)	1.503(6)
C36–O4	1.437(3)	1.439(3)	1.432(2)	1.437(5)	1.451(3)	1.440(5)
O4–C37	1.375(3)	1.364(3)	1.3808(18)	1.369(5)	1.363(3)	1.359(5)
C1–C40	1.485(4)	1.485(4)	1.492(2)	1.478(6)	1.484(4)	1.479(5)
N1–Cu–I	–	–	–	134.06(10)	136.54(7)	139.10(8)
N2–Cu–I	–	–	–	140.52(10)	137.40(8)	133.86(8)
N1–Cu–N2	–	–	–	82.46(14)	83.17(10)	82.55(12)
C1–N1–Cu	–	–	–	131.5(3)	131.5(2)	131.3(3)
C5–N1–Cu	–	–	–	107.6(3)	109.0(2)	108.0(2)
C9–N2–Cu	–	–	–	108.8(3)	109.3(2)	108.0(2)
C12–N2–Cu	–	–	–	131.0(3)	130.7(2)	130.4(3)
C1–N1–Cu	–	–	–	131.5(3)	131.5(2)	131.3(3)
C5–N1–Cu	–	–	–	107.6(3)	109.0(2)	108.0(2)
C9–N2–Cu	–	–	–	108.8(3)	109.3(2)	108.0(2)
C12–N2–Cu	–	–	–	131.0(3)	130.7(2)	130.4(3)
C1–N1–C5	118.8(2)	118.7(2)	119.25(12)	119.1(4)	118.3(3)	119.1(3)
C9–N2–C12	118.9(2)	118.6(2)	119.25(12)	118.6(4)	118.5(3)	119.4(3)
C16–O1–C19	118.8(2)	119.55(19)	117.72(12)	118.1(3)	118.7(3)	117.8(3)
C24–O2–C25	117.1(2)	117.10(19)	118.10(11)	117.7(3)	116.7(2)	116.2(3)
C29–O3–C31	117.5(2)	116.59(19)	118.10(11)	116.6(3)	118.7(2)	117.6(3)
C36–O4–C37	117.4(2)	117.89(19)	117.72(12)	118.7(3)	116.7(2)	120.8(3)
Sum of angles N–Cu–N/I	–	–	–	357.04	357.11	355.51
Cu···phen[D]	–	–	–	0.630	0.462	0.603
I···phen[D]	–	–	–	1.989	1.651	2.067
CuIN1N2 vs phen[E]	–	–	–	29.14	24.33	30.97
N1–C1–C40–C41	−29.24	−19.32	−19.97	26.05	37.92	21.94
N2–C12–C13–C18	−18.75	10.67	19.97	−26.01	−32.40	−24.83
Plane A vs phen[F]	19.04	9.59	20.97	23.09	32.67	26.65
Plane B vs phen[F]	59.62	25.29	1.09	33.50	2.28	44.68
Plane C vs phen[F]	30.43	19.59	20.97	−22.78	−36.02	−20.48
O1···O4	10.365	11.136	10.372	10.747	10.850	10.746
O2···O3	4.768	7.316	4.634	4.758	7.350	4.849
N1···O3	10.746	13.105	10.223	10.670	12.619	11.996
N2···O2	10.642	12.714	10.223	11.534	12.201	10.496
N1···C^{G}_{distal}	10.886	12.696	9.519 (8.487)	11.618	11.955	11.953
N2···C^{G}_{distal}	11.054	12.634	9.519 (8.487)	11.751	12.119	11.451
O1···O3	10.331	12.644	10.176	7.835	12.998	11.509
O2···O4	8.426	11.574	10.176	11.834	10.230	8.036
C17···C42	6.630	6.935	6.379	6.808	7.110	6.710
Void volume	20	474	354	344	482	155

[A]This structure was described earlier in reference [6].
[B]Some or all of the solvate molecules were removed during refinement as described in the Experimental section.
[C]The second value is for the atoms C211, C221, C331, and C341 of the same arene ring.
[D]The distance from the $C_{12}N_2$ least-squares plane.
[E]The angle defined by the CuIN1N2 least-squares plane and the $C_{12}N_2$ least-squares plane.
[F]These represent the absolute values of the angles between the $C_{12}N_2$ least-squares plane and those of the arene ring containing C13–C16 (plane A), the dihydroxyarene (plane B), and the arene ring containing C37–C40 (plane C).
[G]The carbon atoms distal to N1 and N2 are taken as C29 and C25 (**3a**), C301 and C303 (**3b**), and C25 and C29 (C26 and C28, values in parenthesis) (**3c**), respectively; the analogous atoms are employed for **4a**–**c**.

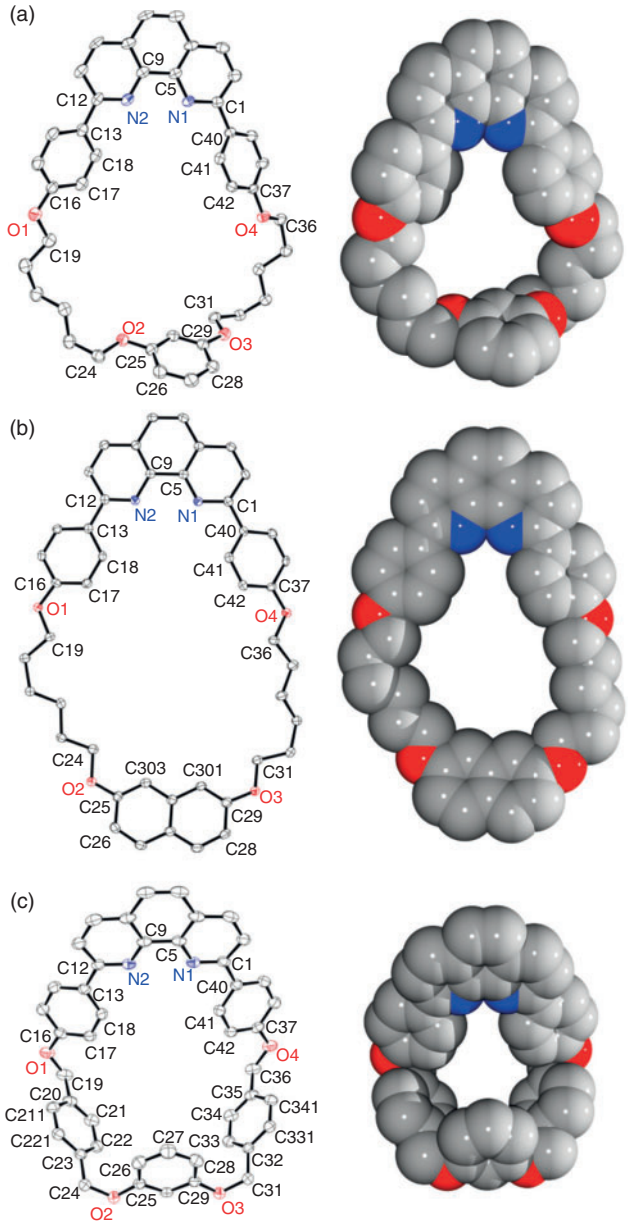

Fig. 2. Thermal ellipsoid plots (50 % probability levels) and space filling representations of the molecular structures of (a) **3a**, (b) **3b**, and (c) **3c**. With the last two, solvent molecules are either omitted or removed during refinement. Hydrogen atoms are omitted for clarity.

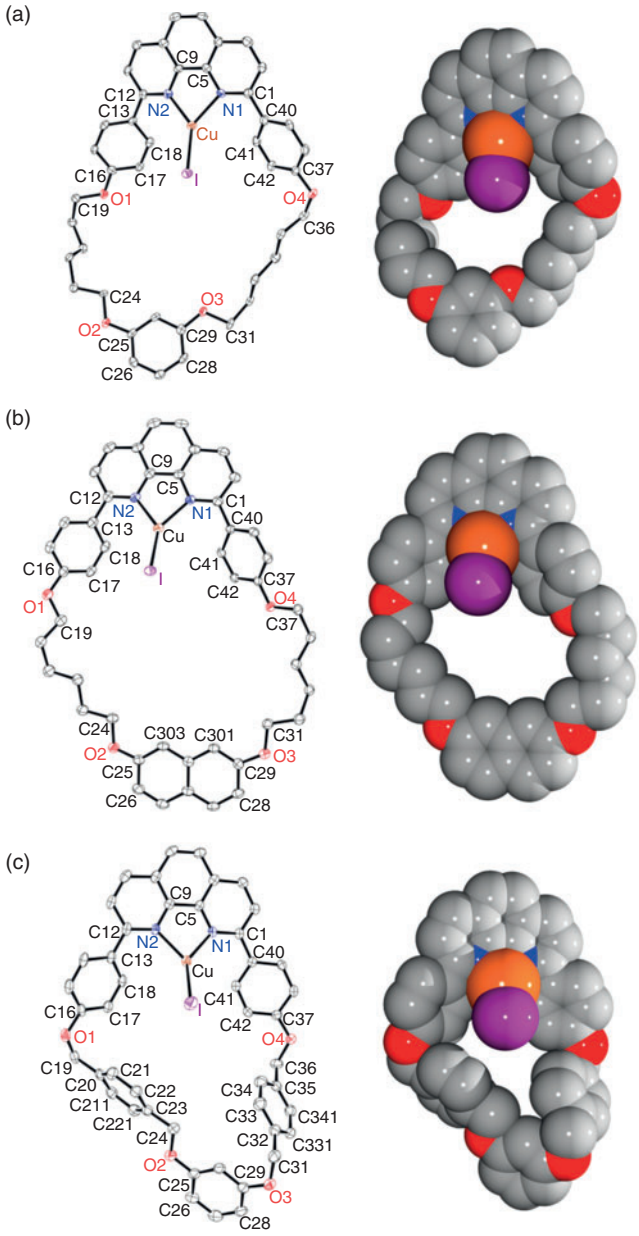

Fig. 3. Thermal ellipsoid plots (50 % probability levels) and space filling representations of the molecular structures of (a) **4a**, (b) **4b**, and (c) **4c**; solvate molecules and hydrogen atoms are omitted for clarity.

4a–**c**, it can be anticipated that the optimized structures closely model those of the real compounds. These data are presented in the Supplementary Material.

Discussion

The syntheses of **2a**–**d** and **3a**–**d** (Schemes 2 and 3) illustrate the versatility of the Williamson ether synthesis for the assembly of macrocycles. With regard to **2a**–**d** and related bis(ethers) described in the Supplementary Material, the highest yields were obtained in reactions with the aliphatic α,ω-dibromide Br $(CH_2)_6$Br (41–47 %) as opposed to reactions with xylylyl dibromides (21–38 %). Possible side reactions include the participation of both primary bromide atoms in ether formation and the generation of dimeric macrocycles derived from two molecules of **1** and two molecules of **2a**–**d**. A weak peak of twice the theoretical mass (+1) was noticed in the mass spectrum of **3d**. However, no traces of a second species could be found by NMR analysis.

The structures of **4a**–**c** differ significantly from those obtained from reactions between 1,10-phenanthroline and CuI. The latter educts react in acetonitrile to give a dimeric complex with bridging iodide ligands and a distorted tetrahedral coordination environment.[19] The copper atoms lie in the plane of the phenanthroline ligand; the Cu–I vectors define angles of 53.5°–65.6° (two different solvates) with the plane. These features are closely modelled by DFT calculations, analogous to those described above (59.7° plane/Cu–I vector angle; D_{2h} symmetry). A solvothermal synthesis affords a polymeric allotrope with a zig-zag $(Cu–I–Cu–I–)_n$ chain and similar tetrahedral copper coordination geometry.[20]

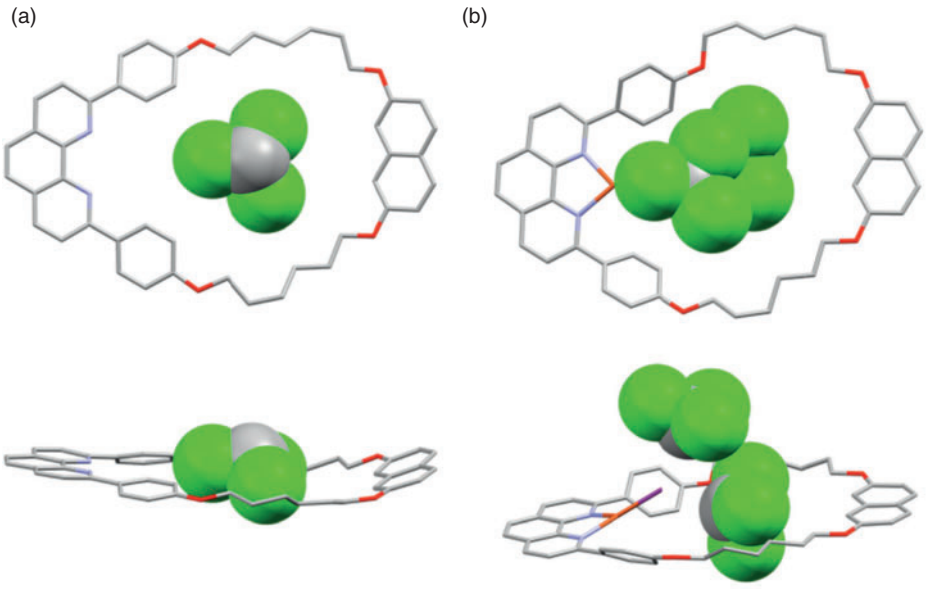

Fig. 4. Representations of crystal structures with solvate molecules included: (a) **3b** with one of the two $CHCl_3$ molecules; (b) **4b** with both $CHCl_3$ molecules.

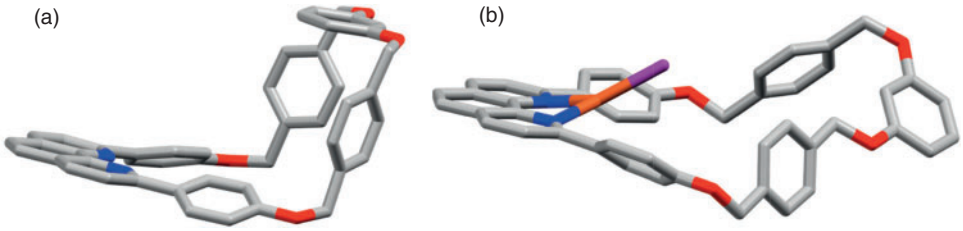

Fig. 5. Folding of (a) the free macrocycle **3c** (empty 'taco shell') and (b) the more opened conformation of the corresponding CuI complex **4c** (stuffed taco). Solvate molecules have been omitted in both cases.

However, the CuI adduct of 2,9-bis(*t*-butyl)-1,10-phenanthroline crystallizes as a monomer, with the copper and iodine atoms markedly removed from the plane of the phenanthroline ligand (0.72 Å and 2.32 Å versus 0.46–0.63 Å and 1.65–2.07 Å for **4a**–**c**).[21] Thus, 2,9-substituents can sterically interfere with in-plane copper coordination. This effect is not conducive to rotaxane syntheses as it renders it more difficult for the two alkynyl coupling partners to interact effectively from opposite faces of the phenanthroline moiety. These data suggest that macrocycles based on 3,8-disubstituted 1,10 phenanthrolines may be more effective for 'active metal template' rotaxane syntheses.[12]

Evaluation of the void space available within the macrocycles of **3a**–**c** and **4a**–**c** was desirable. This was performed, *after removing all solvate molecules*, with the program *Mercury*,[22] using a probe volume of 7.24 $Å^3$, a probe radius of 1.2 Å, and a grid spacing of 0.7 Å. The macrocycle **3a**, the crystal of which did not incorporate any solvent, exhibited a void volume of 20 $Å^3$ (Table 2). In contrast, **3b** and **3c**, which crystallized as a disolvate and monosolvate, respectively, gave void volumes of 474 and 354 $Å^3$. With **4a**–**c**, the largest void volume was associated with the complex that crystallized as a disolvate (**4b**, 482 $Å^3$). The voids in the complexes that were monosolvates were smaller (**4a**, 344 $Å^3$; **4c**, 155 $Å^3$).

In addition to the void volumes displaying a correlation to the number of solvent molecules originally present, they reflect various geometric parameters such as the dimensions of rigid units, folding, and the efficiency of crystal packing. For example, the 'southern hemisphere' of **3b** features a 2,7-dioxanaphthalene moiety, the oxygen-to-oxygen 'wingspan' of which is 7.316 Å (O2···O3). Accordingly, **3b** exhibits a larger void volume than **3a**, **c**, which contain 1,3-OC_6H_4O moieties with oxygen-to-oxygen wingspans of 4.768–4.634 Å (corresponding to a reduction of 35–37 %). However, the rigor of this comparison is compromised by the different number of solvent molecules present in each crystal.

Interestingly, in the 'northern hemisphere', the O1···O4 wingspan associated with the C_6H_4O groups bound to the phenanthroline is 7 % greater in **3b** than in **3c** (11.136 versus 10.372 Å). These and a variety of related data are compiled in the final series of entries in Table 2. For example, the distances between the nitrogen donor atoms in **3b** and opposing aromatic carbon atoms in the 'southern hemisphere' are 12.696–12.634 Å. The corresponding distances for **3a**, **c** are shorter i.e. 11.054–10.886 Å (corresponding to a reduction of 13–14 %) and 9.519–8.487 Å (corresponding to a reduction of 25–33 %), respectively.[23] The corresponding distances in the CuI complexes **4a**–**c** are much more comparable (Table 2).

In the crystal, **3c** exhibits a motif that is reminiscent of the framework of a hard taco shell (Fig. 5a). These motifs stack on top of each other, thus creating extended tunnel-like voids as represented in Fig. 6. In contrast, in the corresponding complex

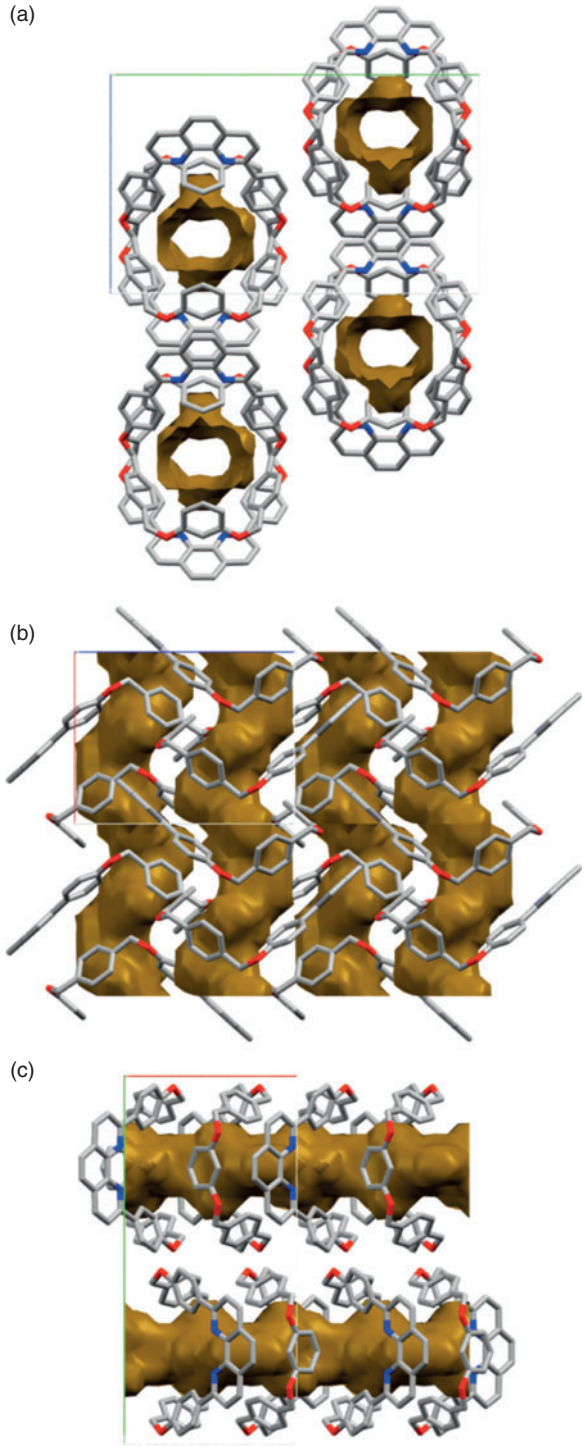

Fig. 6. Tunnel-like voids in the crystal structure of the free macrocycle **3c** after removal of solvate molecules: view along the (a) *a*-, (b) *b*-, and (c) *c*-axes, respectively.

4c, which is also a monosolvate, the CuI moiety intrudes into the less severely folded macrocycle cavity. Accordingly, the void volume decreases by more than 50 % (344 versus 155 $Å^3$). Regardless, despite the intrinsically qualitative nature of these void volume comparisons, they help to define the dimensional limits that can be realized with these macrocycles in MIMs. Additional crystallographic features of ancillary interest are illustrated in figures in the Supplementary Material.

In conclusion, this study has optimized and extended Williamson ether syntheses that enable access to a variety of macrocycles based on the 2,9-bis(4-hydroxyphenyl)-1,10-phenanthroline building block **1**. The corresponding CuI complexes have been prepared, which, as described elsewhere, serve as 'active metal template' precursors to rotaxanes derived from the oxidative homocoupling of terminal alkynes.[5] The structural properties of all of these compounds, as well as the NMR properties of the uncomplexed macrocycles, have been characterized in detail. These data provide a solid foundation for the analysis and interpretation of a variety of properties of the resulting rotaxanes, which include MIMs derived from diplatinum polyynediyl complexes. These efforts will soon be detailed in a comprehensive full paper.[13]

Experimental

General Data

Organic reactions were conducted under ambient conditions, and the copper complexes were prepared under nitrogen atmospheres using Schlenk techniques. Prior to use, THF (Fisher Scientific) was dried using a Glass Contour solvent purification system. Other chemicals CH_2Cl_2, $CHCl_3$, methanol (MeOH) (EMD), acetone, hexanes, ethyl acetate (BDH), $CDCl_3$ (Cambridge Isotope Laboratories), K_2CO_3 (anhydrous, BDH), CuI (99.998 %, Alfa Aesar), 2,7-dihydroxynaphthalene (97 %, Alfa Aesar), 1,6-dibromohexane (97 %, Alfa Aesar), resorcinol (99 %, Alfa Aesar), 1,4-bis(bromomethyl)benzene (97 %, Alfa Aesar), 1,3-bis(bromomethyl)benzene (97 %, Alfa Aesar), silica (40–63 μm, 230–400 mesh, Silicycle), and alumina (neutral, Brockmann I, 50–200 μm, Acros) were used as received. Thin layer chromatography (TLC) was carried out on EMD silica gel 60 F254 or EMD aluminium oxide 60 F254 (neutral) plates that were visualized with 254 nm or 365 nm UV light.

NMR spectra were recorded on a Varian NMRS 500 MHz (ambient probe temperatures) or a Bruker Avance III 500 MHz (cryoprobe conditions) spectrometers and referenced as follows (δ, ppm): ^{1}H, residual internal $CHCl_3$ (7.26); $^{13}C\{^1H\}$, internal $CDCl_3$ (77.16). Mass spectra were recorded on a Thermo Scientific LCQ-DECA (atmospheric pressure chemical ionization (APCI) conditions) or an Applied Biosystems PE SCIEX QSTAR (electrospray ionization (ESI) conditions) spectrometers. Ion assignments were verified against calculated isotope patterns.[24] Melting points were determined on a Stanford Research Systems (SRS) MPA100 (Opti-Melt) automated device. Microanalyses were conducted by Atlantic Microlab.

*2,7-Bis(6-bromohexyloxy)naphthalene (**2b**)*

A round-bottom flask was charged with acetone solutions (96 mL total) of 2,7-dihydroxynaphthalene (3.850 g, 24.04 mmol) and 1,6-dibromohexane (17.594 g, 72.112 mmol) and fitted with a condenser. Then, K_2CO_3 (8.306 g, 60.09 mmol) was added with stirring. The mixture was refluxed. After 3 days, the solvent was removed by rotary evaporation. Water (250 mL) was added. The residue was extracted with CH_2Cl_2 (1200 mL total). The extract was washed with aqueous NaOH (200 mL, 10 % w/v) and brine (200 mL) and dried over Na_2SO_4. The solvent was removed by rotary evaporation. The residue was chromatographed (silica gel, 6.5 cm × 31 cm column, packed in hexanes and eluted with a CH_2Cl_2/hexanes gradient). The solvent was removed from the product containing fractions (assayed by TLC, eluent 1 : 2 v/v CH_2Cl_2/hexanes) by rotary evaporation to give **2b** as a white crystalline solid (4.831 g, 9.934 mmol, 41 %),

mp 74°C. δ_H ($CDCl_3$, 500 MHz) 7.64 (2H, d, $^3J_{HH}$ 8.9, OCCHC*H*), 7.03 (2H, d, $^4J_{HH}$ 2.4, OCC*H*C), 6.98 (2H, dd, $^3J_{HH}$ 8.9, $^4J_{HH}$ 2.4, OCC*H*CH), 4.06 (4H, t, $^2J_{HH}$ 6.4, OCH_2), 3.44 (4H, t, $^2J_{HH}$ 6.8, BrCH_2), 1.94–1.83 (8H, 2 overlapping m, OCH_2CH_2, BrCH_2CH_2), 1.58–1.51 (8H, m, O$CH_2CH_2CH_2$, Br$CH_2CH_2CH_2$). δ_C ($CDCl_3$, 125 MHz) 157.7 (s, O*C*CH), 136.1, 129.2, 124.3, 116.4, 106.1 (5 × s, aryl), 67.8 (s, OCH_2), 34.0, 32.8, 29.2, 28.1, 25.5 (5 × s, O$CH_2CH_2CH_2$, Br$CH_2CH_2CH_2$). *m/z* (APCI$^+$)[25] 487 (100 %, [**2b** + 1]$^+$), 407 (3 %, [**2b** − Br]$^+$), 161 (20 %, [dihydroxynaphthalene + 1]$^+$). Anal. Calc. for $C_{22}H_{30}Br_2O_2$ (486.2870): C 54.34, H 6.22, Br 32.86. Found: C 54.29, H 6.11, Br 32.78 %.

*1,3-Bis(4-bromomethylbenzyloxy)benzene (**2c**)*

A round-bottom flask was charged with a solution of resorcinol (1.016 g, 9.229 mmol) in acetone (15 mL) and fitted with a condenser. Then, K_2CO_3 (3.189 g, 23.21 mmol) was added with stirring, followed by a solution of 1,4-bis(bromomethyl)benzene (7.309 g, 27.69 mmol) in acetone (25 mL). The mixture was refluxed in the dark. After 3.5 days, the solvent was removed by rotary evaporation. Water (200 mL) was added. The mixture was extracted with ethyl acetate (400 mL). The extract was washed with aqueous NaOH (10 % w/v) and dried over $MgSO_4$. The solvent was removed by rotary evaporation. The residue was chromatographed (silica gel, 4.5 cm × 23 cm, packed in hexanes and eluted with a CH_2Cl_2/hexanes gradient 10 : 90 → 20 : 80 → 30 : 70 → 40 : 60 → 50 : 50 v/v). The solvent was removed from the product containing fractions (assayed by TLC, eluent both 1 : 2 and 2 : 1 v/v CH_2Cl_2/hexanes) by rotary evaporation to give **2c** as a white powder (0.928 g, 1.95 mmol, 21 %), mp 107.7–111.8°C. δ_H ($CDCl_3$, 500 MHz) 7.41 (8H, br s, *p*-C_6H_4), 7.20 (1H, t, $^3J_{HH}$ 7.2, OCCHC*H*), 6.58–6.57 (2H, m, OCC*H*CH), 6.60 (1H, m, OCC*H*CO), 5.03 (4H, s, OCH_2), 4.51 (4H, s, BrCH_2). δ_C ($CDCl_3$, 125 MHz) 160.0 (s, O*C*CH), 137.6, 137.4, 130.1 (3 × s, aryl), 129.4, 128.0 (2 × s, *C*H of *p*-C_6H_4), 107.6, 102.4 (2 × s, aryl), 69.7 (s, OCH_2), 33.3 (s, BrCH_2). *m/z* (ESI$^+$)[25] 538 (16 %, [**2c** + 62]$^+$), 477 (7 %, [**2c** + 1]$^+$). Anal. Calc. for $C_{22}H_{20}Br_2O_2$ (476.2076): C 55.49, H 4.23. Found: C 55.22, H 4.13 %.

*1,3-Bis(3-bromomethylbenzyloxy)benzene (**2d**)*

A round-bottom flask was charged with resorcinol (2.565 g, 23.30 mmol), 1,3-bis(bromomethyl)benzene (18.449 g, 69.896 mmol), and acetone (93 mL) and fitted with a condenser. Then, K_2CO_3 (8.050 g, 58.25 mmol) was added with stirring. The mixture was refluxed in the dark. After 3 days, the solvent was removed by rotary evaporation. Water (200 mL) was added. The mixture was extracted with ethyl acetate (7 × 100 mL). The extract was washed with aqueous NaOH (100 mL, 10 % w/v) and brine (200 mL) and dried over $MgSO_4$. The solvent was removed by rotary evaporation. The residue was chromatographed (silica gel, 4.5 cm × 25 cm, packed in hexanes, eluted with a CH_2Cl_2/hexanes gradient 5 : 95 → 20 : 80 v/v). The solvent was removed from the product containing fractions (assayed by TLC, eluent 1 : 2 v/v CH_2Cl_2/hexanes) by rotary evaporation to give **2d** as a white solid (4.190 g, 8.799 mmol, 38 %), mp 74.7–79.8°C. δ_H ($CDCl_3$, 500 MHz) 7.47 (2H, br s, $CH_2CCHCCH_2$), 7.36 (6H, br, $BrCH_2CCHCHCH$) 7.21 (1H, t, $^3J_{HH}$ 8.2, OCCHC*H*), 6.63 (1H, t, $^4J_{HH}$ 2.1, OCC*H*CO), 6.61 (2H, dd, $^3J_{HH}$ 8.1, $^4J_{HH}$ 2.2, OCC*H*CH), 5.04 (4H, s, OCH_2), 4.52 (4H, s, BrCH_2). δ_C ($CDCl_3$, 125 MHz) 160.0 (s, O*C*CH), 138.3, 137.8, 130.2, 129.2, 128.8, 128.2, 127.6, 107.6, 102.3 (9 × s, aryl), 69.8 (s, OCH_2), 33.4 (s, BrCH_2). *m/z* (ESI$^+$)[25] 477 (1 %, [**2d** + 1]$^+$). Anal. Calc. for $C_{22}H_{20}Br_2O_2$ (476.2076): C 55.49, H 4.23. Found: C 54.83, H 4.07 %.

*(2,9-(1,10-Phenanthrolinediyl))(4-$C_6H_4O(CH_2)_6O$)$_2$(2,7-naphthdiyl) (**3b**)*

A round-bottom flask was charged with DMSO solutions (573 mL total) of **2b** (1.393 g, 2.865 mmol) and 2,9-bis (4-hydroxyphenyl)-1,10-phenanthroline (**1**[9a,15]; 1.044 g, 2.865 mmol) that had been neutralized as reported earlier.[9a] Then, K_2CO_3 (5.544 g, 40.11 mmol) and water (5.7 mL) were added with stirring. The sample was stirred at 65°C for 19 h. The solvent was removed by rotary evaporation. Water (100 mL) was added, and the mixture was extracted with CH_2Cl_2 (400 mL). The extract was dried over Na_2SO_4. The solvent was removed by rotary evaporation. The residue was chromatographed (alumina, 4.5 cm × 25 cm column, packed and eluted with CH_2Cl_2). The solvent was removed from the product containing fractions (assayed by TLC, eluent 1 : 1 v/v CH_2Cl_2/hexanes) by rotary evaporation to give **3b** as a moderately light sensitive white solid (1.242 g, 1.803 mmol, 63 %) that was stored in the dark, mp 240°C. δ_H ($CDCl_3$, 500 MHz) 8.43 (4H, d, $^3J_{HH}$ 8.8, H_o),[26] 8.25 (2H, d, $^3J_{HH}$ 8.4, H_4 or H_7),[26] 8.08 (2H, d, $^3J_{HH}$ 8.4, H_3 or H_8),[26] 7.73 (2H, s, H_5 or H_6),[26] 7.65 (2H, d, $^3J_{HH}$ 8.9, OCCHC*H* of naphthyl), 7.12 (2H, d, $^4J_{HH}$ 2.4, OCC*H*CC), 7.11–7.09 (4H, dm, $^3J_{HH}$ 8.8, H_m),[26] 7.00 (2H, dd, $^3J_{HH}$ 8.9, $^4J_{HH}$ 2.4, OCC*H*CH of naphthyl), 4.14 (4H, t, $^3J_{HH}$ 6.8, OCH_2), 4.08 (4H, t, $^3J_{HH}$ 6.4, O′C′H_2), 1.96 (4H, overlapping p, $^3J_{HH}$ 6.5, OCH_2CH_2), 1.90 (4H, overlapping p, $^3J_{HH}$ 6.7, O′C′H_2C′$\underline{H_2}$), 1.67–1.60 (8H, m, $OCH_2CH_2CH_2$, O′C′H_2C′H_2C′$\underline{H_2}$). δ_C ($CDCl_3$, 125 MHz) 160.6, 157.8, 156.5, 146.1, 136.9, 136.1, 132.1, 129.2, 129.1, 127.6, 125.7, 124.3, 119.3, 116.8, 114.8, 105.8 (16 × s, aryl), 68.3, 67.4 (2 × s, OCH_2, O′*C*′H_2), 29.5, 29.1 (2 × s, OCH_2CH_2, O′C′H_2C′H_2), 26.0, 25.7 (2 × s, $OCH_2CH_2CH_2$, O′C′H_2C′H_2C′H_2). *m/z* (ESI$^+$)[25] 689 (100 %, [**3b** + 1]$^+$). Anal. Calc. for $C_{46}H_{44}N_2O_4$ (688.8664): C 80.20, H 6.44, N 4.07. Found: C 79.70, H 6.26, N 4.12 %.

*(2,9-(1,10-Phenanthrolinediyl))(4-$C_6H_4OCH_2$-4-$C_6H_4CH_2O$)$_2$(1,3-C_6H_4) (**3c**)*

A round-bottom flask was charged with DMSO solutions (210 mL total) of **2c** (0.501 g, 1.05 mmol) and **1** (0.383 g, 1.05 mmol) that had been neutralized as reported earlier.[9a] Then, K_2CO_3 (0.435 g, 3.15 mmol) and water (2.1 mL) were added with stirring. The sample was stirred at 65°C in the dark for 4 h. The solvent was removed by rotary evaporation. Water (50 mL) was added, and the mixture was extracted with CH_2Cl_2 (5 × 50 mL). The extract was washed with water (2 × 50 mL) and brine (50 mL) and dried over $MgSO_4$. The solvent was removed by rotary evaporation. The residue was chromatographed (silica gel, 3 cm × 26 cm, packed in CH_2Cl_2, eluted with MeOH/CH_2Cl_2 gradient 1 : 999 → 2 : 998 v/v). The solvent was removed from the product containing fractions (assayed by TLC, eluent 1 : 99 v/v MeOH/CH_2Cl_2) by rotary evaporation to give **3c** as a moderately light sensitive very pale yellow powder (0.278 g, 0.410 mmol, 39 %) that was stored in the dark and darkened slightly at 115°C and melted at 165°C. δ_H ($CDCl_3$, 500 MHz) 8.33 (4H, dm, $^3J_{HH}$ 8.8, H_o),[26] 8.26 (2H, d, $^3J_{HH}$ 8.4, H_4 or H_7),[26] 8.07 (2H, d, $^3J_{HH}$ 8.4, H_3 or H_8),[26] 7.73 (2H, s, H_5 or H_6),[26] 7.36 (8H, br, *p*-$C_6H_4CH_2O$), 7.17 (1H, t, $^3J_{HH}$ 8.2, OCCHC*H* of *m*-$C_6H_4O_2$), 7.11 (4H, d, $^3J_{HH}$ 8.8, H_m),[26] 6.59

(2H, dd, $^3J_{HH}$ 8.2, $^4J_{HH}$ 2.3, OCC*H*CH of *m*-$C_6H_4O_2$), 6.41 (1H, t, $^4J_{HH}$ 2.3, OCC*H*CO), 5.32 (4H, s, OCH_2), 5.07 (4H, s, O′C′H_2). δ_C ($CDCl_3$, 125 MHz) 160.3, 159.8, 156.3, 145.8, 137.3, 136.9, 136.5, 129.9, 129.1, 127.5, 127.3, 126.6, 125.7, 119.5, 116.0, 107.9, 103.0 (17 × s, aryl), 70.2, 69.8 (2 × s, OCH_2, O′C′H_2). *m/z* (ESI$^+$)[25] 679 (100 %, [**3c** + 1]$^+$). Anal. Calc. for $C_{46}H_{34}N_2O_4$ (678.7870): C 81.40, H 5.05, N 4.13. Calc. for $C_{46}H_{34}N_2O_4{\cdot}H_2O$ (696.8022): C 79.29, H 5.21, N 4.02. Found: C 79.30, H 5.16, N 3.97 %.[27]

*(2,9-(1,10-Phenanthrolinediyl))(4-$C_6H_4OCH_2$-3-$C_6H_4CH_2O)_2$(1,3-C_6H_4) (**3d**)*

A round-bottom flask was charged with DMSO solutions (422 mL total) of **2d** (1.005 g, 2.109 mmol) and **1** (0.769 g, 2.110 mmol) that had been neutralized as reported earlier.[9a] Then, K_2CO_3 (2.187 g, 15.82 mmol) and water (4.2 mL) were added with stirring. The sample was stirred at 65°C in the dark for 5 h. The solvent was removed by rotary evaporation. Water (300 mL) was added and the mixture was extracted with CH_2Cl_2 (6 × 100 mL). The extract was washed with brine (100 mL) and water (100 mL) and dried over Na_2SO_4. The solvent was removed by rotary evaporation. The residue was chromatographed (silica gel, 4.5 cm × 25 cm, packed in CH_2Cl_2, eluted with a MeOH/CH_2Cl_2 gradient 1 : 999 → 2:998 → 3 : 997 v/v). The solvent was removed from the product containing fractions (assayed by TLC, eluent 1 : 99 v/v MeOH/CH_2Cl_2) by rotary evaporation to give **3d** as a moderately light sensitive white solid (0.308 g, 0.454 mmol, 22 %) that was stored in the dark and darkened slightly at 120°C and melted at 161°C. δ_H ($CDCl_3$, 500 MHz) 8.37 (4H, dm, $^3J_{HH}$ 8.9, H_o),[26] 8.24 (2H, d, $^3J_{HH}$ 8.4, H_4 or H_7),[26] 8.05 (2H, d, $^3J_{HH}$ 8.4, H_3 or H_8),[26] 7.72 (2H, s, H_5 or H_6),[26] 7.66 (2H, br s, CH_2CCHC), 7.40–7.34 (6H, m, $CH_2CCHCHCHC$), 7.23 (1H, t, $^3J_{HH}$ 8.2, OCCHC*H* of *m*-$C_6H_4O_2$), 7.16 (4H, dm, $^3J_{HH}$ 8.9, H_m),[26] 6.85 (1H, t, $^4J_{HH}$ 2.4, OCC*H*CO), 6.65 (2H, dd, $^3J_{HH}$ 8.2, $^4J_{HH}$ 2.4, OCC*H*CH of *m*-$C_6H_4O_2$), 5.30 (4H, s, OCH_2), 5.13 (4H, s, O′C′H_2). δ_C ($CDCl_3$, 125 MHz) 160.2, 159.8, 156.5, 146.2, 137.9, 137.6, 136.8, 132.8, 130.1, 129.1, 128.9, 127.6, 126.6, 126.2, 125.7, 119.4, 115.7, 107.4, 102.9 (19 × s, aryl), 69.9, 69.7 (2 × s, OCH_2, O′C′H_2). *m/z* (ESI$^+$)[25] 679 (100 %, [**3d** + 1]$^+$), 757 (9 %, [**3d** + 78]$^+$), 1358 (7 %, [2 × **3d** + 1]$^+$). Anal. Calc. for $C_{46}H_{34}N_2O_4$ (678.7870): C 81.40, H 5.05, N 4.13. Calc. for $C_{46}H_{34}N_2O_4{\cdot}2H_2O$ (714.8175): C 77.29, H 5.36, N 3.92. Found: C 77.58, H 5.34, N 3.99 %.[27]

*(**3b**)CuI (**4b**)*

A solution of CuI (0.140 g, 0.734 mmol) in CH_3CN (14 mL) was transferred via a Teflon cannula to a solution of **3b** (0.505 g, 0.734 mmol) in CH_2Cl_2 (33 mL) in a Schlenk flask. The mixture was stirred in the dark. After 1 h, the solvent was removed by rotary evaporation to give a pale orange solid. The residue was recrystallized from hot CH_2Cl_2 (refrigerator storage). The precipitate was isolated by filtration and dried by oil pump vacuum to give **4b** as a bright orange crystalline solid (0.508 g, 0.577 mmol, 79 %), which darkened slightly (contraction) at 124°C and melted at 226°C. δ_H ($CDCl_3$, 500 MHz) 8.42 (2H, br s, $w_{1/2}$ 27), 8.16 (4H, overlapping br d, $^3J_{HH}$ 7.9, *p*-C_6H_4), 8.12 (2H, overlapping br s, $w_{1/2}$ 23), 7.88 (2H, br s), 7.63 (2H, d, $^3J_{HH}$ 8.8), 7.16 (2H, br s, $w_{1/2}$ 36), 7.13 (4H, br d, $^3J_{HH}$ 7.5, *p*-C_6H_4), 6.97 (2H, br d, $^3J_{HH}$ 8.8), 4.20–4.02 (8H, overlapping br s and t, $^3J_{HH}$ 6.7, OCH_2, O′C′H_2), 2.02–1.82 (8H, br m, OCH_2CH_2, O′C′H_2C′H_2), 1.69–1.56 (8H, br, $OCH_2CH_2CH_2$, O′C′H_2C′H_2C′H_2). δ_C[28] ($CDCl_3$, 125 MHz, cryoprobe) 161.4, 158.6, 157.8, 138.0, 136.3, 131.4, 129.1, 127.6, 126.0, 124.3, 116.8, 115.0, 106.2 (13 × s, aryl), 68.1, 67.5 (2 × s, OCH_2, O′C′H_2), 29.2, 28.9 (2 × s, OCH_2CH_2, O′C′H_2C′H_2), 25.6, 25.5 (2 × s, $OCH_2CH_2CH_2$, O′C′H_2C′H_2C′H_2). *m/z* (ESI$^+$)[25] 751 (60 %, [(**3b**)Cu]$^+$), 689 (100 %, [**3b** + 1]$^+$). Anal. Calc. for $C_{46}H_{44}CuIN_2O_4$ (879.3168): C 62.83, H 5.04, N 3.19. Found: C 63.38, H 5.34, N 3.13 %.

*(**3c**)CuI (**4c**)*

A solution of CuI (0.035 g, 0.18 mmol) in CH_3CN (3.5 mL) and a solution of **3c** (0.035 g, 0.18 mmol) in CH_2Cl_2 (8 mL) were combined using the same procedure as that used for preparing **4b** (3 h stirring). An identical workup gave **4c** as a pale orange solid (0.061 g, 0.073 mmol, 40 %), mp 107.7–111.8°C. *m/z* (ESI$^+$) 741 (50 %, [(**3c**)Cu]$^+$), 679 (100 %, [**3c** + 1]$^+$). *m/z* (ESI$^-$) 127 (100 %, [I]$^-$). Anal. Calc. for $C_{46}H_{34}CuIN_2O_4$ (869.2374): C 63.56, H 3.94, N 3.22. Calc. for $C_{46}H_{34}CuIN_2O_4{\cdot}CH_2Cl_2$ (954.1643): C 59.16, H 3.80, N 2.94. Found C 60.04, H 3.92, N 2.90 %.[29]

*(**3d**)CuI (**4d**)*

A solution of CuI (0.019 g, 0.098 mmol) in CH_3CN (1 mL) and a solution of **3d** (0.067 g, 0.098 mmol) in CH_2Cl_2 (4 mL) were combined using the same procedure as that used for preparing **4b** (0.5 h stirring). The precipitate was isolated by filtration and dried by oil pump vacuum to give **4d** as a yellow solid (0.068 g, 0.078 mmol, 80 %), mp 107.7–111.8°C. Anal. Calc. for $C_{46}H_{34}CuIN_2O_4$ (869.2374): C 63.56, H 3.94, N 3.22. Calc. for $C_{46}H_{34}CuIN_2O_4{\cdot}CH_2Cl_2{\cdot}0.75H_2O$ (967.6758): C 58.34, H 3.91, N 2.89. Found: C 58.59, H 4.01, N 2.92 %.[30]

Crystallography A

A CH_2Cl_2 solution of **3a** was allowed to evaporate slowly at room temperature. After 3 days, the resulting colourless plates were analyzed as outlined in Table 1. Cell parameters were obtained from 1080 frames using a 0.5° scan[31] and refined with 24948 reflections. Integrated intensity information for each reflection was obtained by reduction of the data frames with *APEX2*.[32] The integration method employed a three-dimensional profiling algorithm. All data were corrected for Lorentz and polarization factors as well as crystal decay effects. *SADABS* was used for absorption corrections.[33] The space group was determined from systematic reflection conditions and statistical tests. The structure was solved by direct methods using *SHELXTL* (SHELXS).[34] Non-hydrogen atoms were refined with anisotropic thermal parameters. Hydrogen atoms were placed in idealized positions and refined using a riding model. The structure was refined (weighted least-squares refinement on F^2) to convergence.[34] The absence of additional symmetry or voids was confirmed using *PLATON* (ADDSYM).[35]

Crystallography B

A $CHCl_3$ solution of **3b** was allowed to evaporate slowly at room temperature. After 3 days, the resulting colourless prisms were analyzed as outlined in Table 1. Cell parameters were obtained from 180 frames using a 0.5° scan.[31] Integrated intensity information for each reflection was obtained by reduction of the data frames with the program *APEX2*.[32] *SADABS* was used for absorption corrections.[33] The space group was determined from systematic reflection conditions and statistical tests.

Table 3. Crystallographic data for 4a–c

	4a·CH_2Cl_2	**4b**·$2CHCl_3$	**4c**·CH_2Cl_2
Empirical formula	$C_{43}H_{44}Cl_2CuIN_2O_4$	$C_{48}H_{46}Cl_6CuIN_2O_4$	$C_{47}H_{36}Cl_2CuIN_2O_4$
Formula weight	914.14	1118.01	954.12
Temperature [K]	110(2)	110(2)	110(2)
Wavelength [Å]	1.54178	0.71073	0.71073
Diffractometer	Bruker D8 GADDS	Bruker APEX 2	Bruker APEX 2
Crystal system	Monoclinic	Triclinic	Triclinic
Space group	*P*2(1)/*c*	*P*-1	*P*-1
Unit cell dimensions			
a [Å]	13.8010(10)	11.888(3)	7.5981(2)
b [Å]	8.1146(7)	14.904(4)	12.5786(2)
c [Å]	35.376(2)	14.905(4)	21.1089(4)
α [°]	90	112.140(7)	82.7280(10)
β [°]	95.820(4)	102.331(7)	88.1180(10)
γ [°]	90	91.793(6)	80.7170(10)
Volume [Å^3]	3941.3(5)	2371.5(11)	1974.86(7)
Z	4	2	2
ρ_{calcd} [Mg m^{-3}]	1.541	1.566	1.605
μ [mm^{-1}]	8.536	1.495	1.519
F(000)	1856	1128	960
Crystal size [mm^3]	0.13 × 0.11 × 0.02	0.18 × 0.12 × 0.12	0.20 × 0.12 × 0.03
Range for data collection	3.22 to 60.00	1.767 to 27.527	2.39 to 27.56
Index ranges	$-15 \le h \le 15$	$-15 \le h \le 15$	$-9 \le h \le 9$
	$-9 \le k \le 8$	$-19 \le k \le 19$	$-16 \le k \le 16$
	$-39 \le l \le 39$	$-19 \le l \le 19$	$-27 \le l \le 27$
Reflections collected	46266	24046	43439
Independent reflections	5803 ($R_{int} = 0.0878$)	10655 ($R_{int} = 0.0365$)	9006 ($R_{int} = 0.0624$)
Max. and min. transmission	0.8478 and 0.4033	0.7456 and 0.6326	0.9858 and 0.8325
Data / restraints / parameters	5803 / 0 / 478	10655 / 0 / 559	9006 / 9 / 530
Goodness-of-fit on F^2	1.038	1.051	1.034
Final *R* indices [$I > 2\sigma(I)$]	$R1 = 0.0442$	$R1 = 0.0401$	$R1 = 0.0470$
	$wR2 = 0.1104$	$wR2 = 0.0856$	$wR2 = 0.1131$
R indices (all data)	$R1 = 0.0545$	$R1 = 0.0591$	$R1 = 0.0723$
	$wR2 = 0.1141$	$wR2 = 0.0948$	$wR2 = 0.1282$
Largest diff. peak and hole [eÅ^{-3}]	1.034 and −0.836	0.993 and −0.596	1.746 and −1.821

The structure was solved by direct methods using *SHELXTL* (SHELXS).[34] Two $CHCl_3$ molecules were found for each molecule of **3b**. One molecule was successfully modelled (disordered over two positions). The other molecule could not be modelled so the electron density contribution was extracted with the program *PLATON*/*SQUEEZE*.[35] Restraints were used to keep the bond distances and thermal ellipsoids chemically meaningful. Note that the formula and density reported in the CIF file reflect the results using *SQUEEZE*. Non-hydrogen atoms were refined with anisotropic thermal parameters. Hydrogen atoms were placed in idealized positions and refined using a riding model. The structure was refined (weighted least-squares refinement on F^2) to convergence.[34] The absence of additional symmetry or voids was confirmed using *PLATON* (ADDSYM).[35]

Crystallography C

A CH_2Cl_2 solution of **3c** was allowed to evaporate slowly at room temperature. After 4 days, the resulting colourless plates were analyzed as outlined in Table 1. Cell parameters were obtained from 60 frames using a 0.5° scan. Integrated intensity information for each reflection was obtained by reduction of the data frames with the program *APEX2*.[32] *SADABS* was used for absorption corrections.[33] The space group was determined from systematic reflection conditions and statistical tests. The structure was solved by direct methods using *SHELXTL* (SHELXS).[34] One molecule of CH_2Cl_2 was present, however, was disordered and could not be successfully modelled. Thus, the electron density contribution was extracted with the program *PLATON*/*SQUEEZE*.[35] Restraints were used to keep the bond distances and thermal ellipsoids chemically meaningful. Non-hydrogen atoms were refined with anisotropic thermal parameters. Hydrogen atoms were placed in idealized positions and refined using a riding model. The structure was refined (weighted least-squares refinement on F^2) to convergence.[34] The absence of additional symmetry or voids was confirmed using *PLATON* (ADDSYM).[35]

Crystallography D

A CH_2Cl_2 solution of **4a** was allowed to evaporate slowly at room temperature. After 1 day, the resulting red plates were analyzed as outlined in Table3. Cell parameters were obtained from 180 frames using a 0.5° scan.[31] Integrated intensity information for each reflection was obtained by reduction of the data frames with the program *APEX2*.[32] *SADABS* was used for absorption corrections.[33] The space group was determined from systematic reflection conditions and statistical tests. The structure was solved by direct methods using *SHELXTL*

(SHELXS).[34] A CH_2Cl_2 molecule was found for nearly every molecule of **4a** (refined with an occupancy value close to 1). Non-hydrogen atoms were refined with anisotropic thermal parameters. Hydrogen atoms were placed in idealized positions and refined using a riding model. The structure was refined (weighted least-squares refinement on F^2) to convergence.[34] The absence of additional symmetry or voids was confirmed using *PLATON* (ADDSYM).[35]

Crystallography E

A $CHCl_3$ solution of **4b** was allowed to evaporate slowly at room temperature. After 3 days, the resulting red prisms were analyzed as outlined in Table 3. Cell parameters were obtained from 60 frames using a 0.5° scan.[31] Integrated intensity information for each reflection was obtained by reduction of the data frames with the program *APEX2*.[32] *SADABS* was used for absorption corrections.[33] The space group was determined from systematic reflection conditions and statistical tests. The structure was solved by direct methods using *SHELXTL* (SHELXS).[34] Two $CHCl_3$ molecules were located and refined for each molecule of **4b**. Non-hydrogen atoms were refined with anisotropic thermal parameters. Hydrogen atoms were placed in idealized positions and refined using a riding model. The structure was refined (weighted least-squares refinement on F^2) to convergence.[34] The absence of additional symmetry or voids was confirmed using *PLATON* (ADDSYM).[35]

Crystallography F

A CH_2Cl_2 solution of **4c** was allowed to evaporate slowly at room temperature. After 3 days, the resulting orange plates were analyzed as outlined in Table 3. Cell parameters were obtained from 60 frames using a 0.5° scan.[31] Integrated intensity information for each reflection was obtained by reduction of the data frames with the program *APEX2*.[32] *SADABS* was used for absorption corrections.[33] The space group was determined from systematic reflection conditions and statistical tests. The structure was solved by direct methods using *SHELXTL* (SHELXS).[34] A disordered CH_2Cl_2 molecule was found for each molecule of **4c** and was successfully modelled by application of a restrained distance and displacement parameter refinement. Non-hydrogen atoms were refined with anisotropic thermal parameters. Hydrogen atoms were placed in idealized positions and refined using a riding model. The structure was refined (weighted least-squares refinement on F^2) to convergence.[34] The absence of additional symmetry or voids was confirmed using *PLATON* (ADDSYM).[35]

DFT Calculations

Computations were performed using the *Gaussian09* program package.[36] Full geometry optimizations and frequency calculations were carried out on macrocycles **3** and their CuI complexes **4** without any symmetry constraints. The B3LYP[37] functional was implemented with the D95V basis set for C, H, N, and O atoms, whereas the LANL2DZDP ECP was used to include the appropriate polarization functions for **I** in **4a–f**. To account for the relativistic effects on Cu, SDD was employed.

Supplementary Material

CCDC nos 950619 and 1508487–1508490 contain the supplementary crystallographic data for this paper. These data can be obtained free of charge via www.ccdc.cam.ac.uk/data_request/cif (or from the Cambridge Crystallographic Data Centre (CCDC), 12 Union Road, Cambridge CB2 1EZ, UK; fax: +44(0) 1223 336033; email: deposit@ccdc.cam.ac.uk). Additional views of the crystal structures, experimental procedures, and Cartesian coordinates are also provided as well as a molecular structure file that can be read by the program *Mercury*[22] and contains the optimized geometries of all computed structures.[38]

Acknowledgements

We thank the US National Science Foundation (grant nos CHE-1153085 and CHE-1566601) for support, the Laboratory for Molecular Simulation and Texas A&M High Performance Research Computing, Mr Joseph S. Villalpando and Mr Alex J. Kalin (undergraduate researchers) for the synthesis of precursors, and Dr Tobias Fiedler for preparing the graphical abstract.

References

[1] C. J. Bruns, J. F. Stoddart, *The Nature of the Mechanical Bond: From Molecules to Machines* **2017** (John Wiley & Sons, Inc.: Hoboken, NJ).

[2] (a) J.-M. Lehn, *Supramolecular Chemistry: Concepts and Perspectives* **1995** (VCH: Weinheim, Germany).
(b) J.-P. Sauvage, C. Dietrich-Buchecker (Eds), *Molecular Catenanes, Rotaxanes and Knots: A Journey Through the World of Molecular Topology* **1999** (Wiley-VCH: Weinheim, Germany).

[3] (a) T. J. Hubin, D. H. Busch, *Coord. Chem. Rev.* **2000**, *200–202*, 5. doi:10.1016/S0010-8545(99)00242-8
(b) R. S. Forgan, J.-P. Sauvage, J. F. Stoddart, *Chem. Rev.* **2011**, *111*, 5434. doi:10.1021/CR200034U
(c) L. F. Lindoy, K.-M. Park, S. S. Lee, *Chem. Soc. Rev.* **2013**, *42*, 1713. doi:10.1039/C2CS35218D
(d) N. H. Evans, P. D. Beer, *Chem. Soc. Rev.* **2014**, *43*, 4658. doi:10.1039/C4CS00029C
(e) G. Gil-Ramírez, D. A. Leigh, A. J. Stephens, *Angew. Chem., Int. Ed.* **2015**, *54*, 6110. doi:10.1002/ANIE.201411619 [*Angew. Chem.* **2015**, *127*, 6208 doi:10.1002/ange.201411619]

[4] (a) M. Pérez-Alvarez, F. M. Raymo, S. J. Rowan, D. Schiraldi, J. F. Stoddart, Z.-H. Wang, A. J. P. White, D. J. Williams, *Tetrahedron* **2001**, *57*, 3799. doi:10.1016/S0040-4020(01)00257-5
(b) D. A. Leigh, A. Venturini, A. J. Wilson, J. K. Y. Wong, F. Zerbetto, *Chem. – Eur. J.* **2004**, *10*, 4960. doi:10.1002/CHEM.200305662
(c) O. Š. Miljanić, W. R. Dichtel, S. I. Khan, S. Mortezaei, J. R. Heath, J. F. Stoddart, *J. Am. Chem. Soc.* **2007**, *129*, 8236. doi:10.1021/JA071319N
(d) V. Aucagne, J. Berná, J. D. Crowley, S. M. Goldup, K. D. Hänni, D. A. Leigh, P. J. Lusby, V. E. Ronaldson, A. M. Z. Slawin, A. Viterisi, D. B. Walker, *J. Am. Chem. Soc.* **2007**, *129*, 11950. doi:10.1021/JA073513F
(e) J. Berná, J. D. Crowley, S. M. Goldup, K. D. Hänni, A.-L. Lee, D. A. Leigh, *Angew. Chem., Int. Ed.* **2007**, *46*, 5709. doi:10.1002/ANIE.200701678 [*Angew. Chem.* **2007**, *119*, 5811 doi:10.1002/ange.200701678]
(f) C. D. Meyer, R. S. Forgan, K. S. Chichak, A. J. Peters, N. Tangchaivang, G. W. V. Cave, S. I. Khan, S. J. Cantrill, J. F. Stoddart, *Chem. – Eur. J.* **2010**, *16*, 12570. doi:10.1002/CHEM.201001806
(g) J. D. Crowley, K. D. Hänni, D. A. Leigh, A. M. Z. Slawin, *J. Am. Chem. Soc.* **2010**, *132*, 5309. doi:10.1021/JA101029U
(h) G. T. Spence, N. G. White, P. D. Beer, *Org. Biomol. Chem.* **2012**, *10*, 7282. doi:10.1039/C2OB26237A
(i) H. Iwamoto, W. Takizawa, K. Itoh, T. Hagiwara, E. Tayama, E. Hasegawa, T. Haino, *J. Org. Chem.* **2013**, *78*, 5205. doi:10.1021/JO400239H
(j) J.-F. Ayme, J. E. Beves, C. J. Campbell, D. A. Leigh, *Chem. Soc. Rev.* **2013**, *42*, 1700. doi:10.1039/C2CS35229J

(k) M. Frasconi, T. Kikuchi, D. Cao, Y. Wu, W.-G. Liu, S. M. Dyar, G. Barin, A. A. Sarjeant, C. L. Stern, R. Carmieli, C. Wang, M. R. Wasielewski, W. A. Goddard, III, J. F. Stoddart, *J. Am. Chem. Soc.* **2014**, *136*, 11011. doi:10.1021/JA504662A

[5] (a) N. Weisbach, Z. Baranová, S. Gauthier, J. H. Reibenspies, J. A. Gladysz, *Chem. Commun.* **2012**, *48*, 7562. doi:10.1039/C2CC33321J
(b) Z. Baranová, H. Amini, N. Bhuvanesh, J. A. Gladysz, *Organometallics* **2014**, *33*, 6746. doi:10.1021/OM501026U

[6] Computational study: H. Sahnoune, Z. Baranová, N. Bhuvanesh, J. A. Gladysz, J.-F. Halet, *Organometallics* **2013**, *32*, 6360. doi:10.1021/OM400709Q

[7] (a) W. Mohr, J. Stahl, F. Hampel, J. A. Gladysz, *Chem. – Eur. J.* **2003**, *9*, 3324. doi:10.1002/CHEM.200204741
(b) Q. Zheng, J. C. Bohling, T. B. Peters, A. C. Frisch, F. Hampel, J. A. Gladysz, *Chem. – Eur. J.* **2006**, *12*, 6486. doi:10.1002/CHEM.200600615
(c) J. Stahl, W. Mohr, L. de Quadras, T. B. Peters, J. C. Bohling, J. M. Martín-Alvarez, G. R. Owen, F. Hampel, J. A. Gladysz, *J. Am. Chem. Soc.* **2007**, *129*, 8282. doi:10.1021/JA0716103
(d) L. de Quadras, E. B. Bauer, W. Mohr, J. C. Bohling, T. B. Peters, J. M. Martín-Alvarez, F. Hampel, J. A. Gladysz, *J. Am. Chem. Soc.* **2007**, *129*, 8296. doi:10.1021/JA071612N
(e) L. de Quadras, E. B. Bauer, J. Stahl, F. Zhuravlev, F. Hampel, J. A. Gladysz, *New J. Chem.* **2007**, *31*, 1594. doi:10.1039/B708690N
(f) G. R. Owen, J. Stahl, F. Hampel, J. A. Gladysz, *Chem. – Eur. J.* **2008**, *14*, 73. doi:10.1002/CHEM.200701268
(g) M. C. Clough, T. Fiedler, N. Bhuvanesh, J. A. Gladysz, *J. Organomet. Chem.* **2016**, *812*, 34. doi:10.1016/J.JORGANCHEM.2015.09.020

[8] A. S. Hay, *J. Org. Chem.* **1962**, *27*, 3320. doi:10.1021/JO01056A511

[9] (a) C. Dietrich-Buchecker, J.-P. Sauvage, *Tetrahedron* **1990**, *46*, 503. doi:10.1016/S0040-4020(01)85433-8
(b) J.-C. Chambron, J.-P. Sauvage, K. Mislow, A. De Cian, J. Fischer, *Chem. – Eur. J.* **2001**, *7*, 4085. doi:10.1002/1521-3765(20011001)7:19<4085::AID-CHEM4085>3.0.CO;2-M
(c) A. Joosten, Y. Trolez, J.-P. Collin, V. Heitz, J.-P. Sauvage, *J. Am. Chem. Soc.* **2012**, *134*, 1802. doi:10.1021/JA210113Y

[10] (a) S. Saito, E. Takahashi, K. Nakazono, *Org. Lett.* **2006**, *8*, 5133. doi:10.1021/OL062247S
(b) Y. Sato, R. Yamasaki, S. Saito, *Angew. Chem., Int. Ed.* **2009**, *48*, 504. doi:10.1002/ANIE.200804864 [*Angew. Chem.* **2009**, *121*, 512]
(c) S. Saito, *J. Inclusion Phenom. Macrocyclic Chem.* **2015**, *82*, 437. doi:10.1007/S10847-015-0511-1
(d) R. Hayashi, Y. Mutoh, T. Kasama, S. Saito, *J. Org. Chem.* **2015**, *80*, 7536. doi:10.1021/ACS.JOC.5B01120
(e) R. Hayashi, Y. Slavík, T. Kasama, S. Saito, *J. Org. Chem.* **2016**, *81*, 1175. doi:10.1021/ACS.JOC.5B02697

[11] (a) L. D. Movsisyan, D. V. Kondratuk, M. Franz, A. L. Thompson, R. R. Tykwinski, H. L. Anderson, *Org. Lett.* **2012**, *14*, 3424. doi:10.1021/OL301392T
(b) L. D. Movsisyan, M. Franz, F. Hampel, A. L. Thompson, R. R. Tykwinski, *J. Am. Chem. Soc.* **2016**, *138*, 1366. doi:10.1021/JACS.5B12049

[12] (a) J. D. Crowley, S. M. Goldup, A. L. Lee, D. A. Leigh, R. T. McBurney, *Chem. Soc. Rev.* **2009**, *38*, 1530. doi:10.1039/B804243H
(b) J. E. Beves, B. A. Blight, C. J. Campbell, D. A. Leigh, R. T. McBurney, *Angew. Chem., Int. Ed.* **2011**, *50*, 9260. doi:10.1002/ANIE.201007963 [*Angew. Chem.* **2011**, *123*, 9428]
(c) J. E. Beves, B. A. Blight, C. J. Campbell, D. A. Leigh, R. T. McBurney, *Angew. Chem.* **2011**, *123*, 9428. doi:10.1002/ANGE.201007963
(d) V. Aucagne, K. D. Hänni, D. A. Leigh, P. J. Lusby, D. B. Walker, *J. Am. Chem. Soc.* **2006**, *128*, 2186. doi:10.1021/JA056903F

[13] Z. Baranová, *Studies of Rotaxanes Consisting of 1,10-Phenanthroline Based Macrocycles and Platinum-Capped Polyynediyl Complexes: A Steric and a Dynamic Approach to Molecular Insulation* **2017**, Ph.D. thesis, Texas A&M University, College Station, Texas, USA.

[14] S. Saito, K. Nakazono, E. Takahashi, *J. Org. Chem.* **2006**, *71*, 7477 (see also the supporting information therein). doi:10.1021/JO060829H

[15] (a) C. O. Dietrich-Buchecker, J. P. Sauvage, *Tetrahedron Lett.* **1983**, *24*, 5091. doi:10.1016/S0040-4039(00)94049-8
(b) C. O. Dietrich-Buchecker, J.-P. Sauvage, *J. Am. Chem. Soc.* **1984**, *106*, 3043. doi:10.1021/JA00322A055

[16] (a) T. Ogawa, T. Kishimoto, K. Kobayashi, N. Ono, *J. Chem. Soc., Perkin Trans. 1* **1998**, 529. doi:10.1039/A705995G
(b) N. Watarai, H. Kawasaki, I. Azumaya, R. Yamasaki, S. Saito, *Heterocycles* **2009**, *79*, 531. doi:10.3987/COM-08-S(D)13

[17] A reviewer has questioned why the yield of **4c** is only 40 %, relative to the higher yield (80 %) obtained for the other CuI complexes. It is thought that the crystallization of this complex is not as efficient, as the mother liquor remains pale orange.

[18] The atom labels for **3a** (Fig. 2) correspond to those in the cif file for the crystal structure of **3a**. In the text, the atoms of **3b**, **c**, and **4a**–**c** have been renumbered to match (Figs. 2 and 3 and Table 2). It should be kept in mind that due to the mirror plane in **3c**, there are fewer unique carbon, nitrogen, and oxygen atoms. Thus, atoms that are equivalent by symmetry bear different numbers. The crystal structure of **3a** has also been reported in an earlier paper, see ref. [6]

[19] (a) P. C. Healy, *J. Chem. Soc., Dalton Trans.* **1985**, 2531. doi:10.1039/DT9850002531
(b) X.-P. Zhou, D. Li, S. W. Ng, *Acta Crystallogr.* **2005**, *E61*, m654.

[20] Y. Yang, W. Chai, L. Song, K. Shu, *Acta Crystallogr.* **2010**, *E66*, m1486.

[21] J. Nitsch, C. Kleeberg, R. Fröhlich, A. Steffen, *Dalton Trans.* **2015**, *44*, 6944. doi:10.1039/C4DT03706E

[22] C. F. Macrae, I. J. Bruno, J. A. Chisholm, P. R. Edgington, P. McCabe, E. Pidcock, L. Rodriguez-Monge, R. Taylor, J. van de Streek, P. A. Wood, *J. Appl. Crystallogr.* **2008**, *41*, 466. doi:10.1107/S0021889807067908

[23] The exact comparisons are as follows: **3a**, N1···C29 10.886 Å and N2···C25 11.054 Å; **3b**, N1···C301 12.696 Å and N2···C303 12.696 Å; **3c**, N1···C29 9.519 Å and N1···C28 8.487 Å; **4a**, N1···C29 11.618 Å and N2···C25 11.751 Å; **4b**, N1···C301 11.955 Å and N2···C303 12.119 Å; **4c**, N1···C29 11.953 Å and N2···C25 11.451 Å.

[24] M. Loos, C. Gerber, F. Corona, J. Hollender, H. Singer, *Anal. Chem.* **2015**, *87*, 5738. doi:10.1021/ACS.ANALCHEM.5B00941 [*enviPat* Web 2.1. Available at http://www.envipat.eawag.ch/index.php (accessed 25 November 2016)].

[25] Each *m*/*z* value corresponds to the most intense peak of the isotope envelope, and the assignments have been verified by simulations.

[26] These ^{1}H NMR assignments are based on those given in reference [9a]. For the numbering or labelling of certain atoms, see Fig. S1.

[27] Traces of H_2O are apparent in the ^{1}H NMR spectrum.

[28] The ^{13}C NMR signals were assigned based on data obtained for a similar macrocycle, see ref. [10a]. The solubility of this compound was very low in most NMR solvents (CD_2Cl_2, $CDCl_3$, C_6D_6, [D8]toluene, CD_3CN) at room temperature, and three signals could not be observed, even in spectra recorded using a cryoprobe.

[29] This compound is not sufficiently soluble for ^{1}H and ^{13}C NMR spectra. However, the crystal (Fig. 3c) is a CH_2Cl_2 monosolvate, and the microanalysis better fits this formula.

[30] This compound is not sufficiently soluble for ^{1}H and ^{13}C NMR spectroscopy analysis that would evaluate the solvation model that fits the data.

[31] G. M. Sheldrick, *Cell_Now (version 2008/1): Program for Obtaining Unit Cell Constants from Single Crystal Data* **2008** (University of Göttingen: Germany).

[32] APEX2, *Program for Data Collection on Area Detectors* **2008** (BRUKER AXS Inc.: Madison, WI).

[33] G. M. Sheldrick, *Program for Absorption Correction of Area Detector Frames* **2012** (BRUKER AXS Inc.: Madison, WI).

[34] G. M. Sheldrick, *Acta Crystallogr.* **2008**, *A64*, 112. doi:10.1107/S0108767307043930

[35] A. L. Spek, *J. Appl. Crystallogr.* **2003**, *36*, 7. doi:10.1107/S0021889802022112

[36] M. J. Frisch, G. W. Trucks, H. B. Schlegel, G. E. Scuseria, M. A. Robb, J. R. Cheeseman, G. Scalmani, V. Barone, B. Mennucci, G. A. Petersson, H. Nakatsuji, M. Caricato, X. Li, H. P. Hratchian, A. F. Izmaylov, J. Bloino, G. Zheng, J. L. Sonnenberg, M. Hada, M. Ehara, K. Toyota, R. Fukuda, J. Hasegawa, M. Ishida, T. Nakajima, Y. Honda, O. Kitao, H. Nakai, T. Vreven, J. A. Montgomery Jr, J. E. Peralta, F. Ogliaro, M. Bearpark, J. J. Heyd, E. Brothers, K. N. Kudin, V. N. Staroverov, R. Kobayashi, J. Normand, K. Raghavachari, A. Rendell, J. C. Burant, S. S. Iyengar, J. Tomasi, M. Cossi, N. Rega, J. M. Millam, M. Klene, J. E. Knox, J. B. Cross, V. Bakken, C. Adamo, J. Jaramillo, R. Gomperts, R. E. Stratmann, O. Yazyev, A. J. Austin, R. Cammi, C. Pomelli, J. W. Ochterski, R. L. Martin, K. Morokuma, V. G. Zakrzewski, G. A. Voth, P. Salvador, J. J. Dannenberg, S. Dapprich, A. D. Daniels, Ö. Farkas, J. B. Foresman, J. V. Ortiz, J. Cioslowski, D. J. Fox, *Gaussian 09, Revision D.01* **2009** (Gaussian, Inc.: Wallingford CT).

[37] (a) A. D. Becke, *J. Chem. Phys.* **1993**, *98*, 5648. doi:10.1063/1.464913 (b) C. Lee, W. Yang, R. G. Parr, *Phys. Rev. B* **1988**, *37*, 785. doi:10.1103/PHYSREVB.37.785

[38] D. L. Lichtenberger, J. A. Gladysz, *Organometallics* **2014**, *33*, 835. doi:10.1021/OM500109U